Time-dependent tensile strengths of Bushveld Complex rocks and implications for rock failure around mining excavations

by D. Nyungu* and T.R. Stacey

Synopsis

Despite observations of spalling and damage of mine excavation wall rock in the Bushveld Complex (BC) over the passage of time, there have been very few time-dependent or creep tests carried out in South Africa on rock, particularly on BC rock types. The research described in this paper deals with the investigation of stress and strain conditions influencing spalling of wall rock in BC mine excavations, and the influence of time on the tensile strength of several BC rock types.

Time-dependent laboratory testing of BC rocks was carried out in indirect tension. The results show that the magnitude of the tensile strength of BC rock types is approximately 5% of their uniaxial compressive strength magnitudes. The average long-term uniaxial compressive strength of the BC rocks, interpreted from the axial stress-volumetric strain graphs, is 56% of the UCS value. The long-term tensile strength is shown to be less than 70% of the normal tensile strength. Extension strains at tensile strength failure ranged between 0.16 and 0.21 millistrain. Values corresponding with the long-term tensile strength are less than 70% of this range, namely, 0.11 to 0.15 millistrain. These results represent new knowledge, since such rock testing and analysis does not appear to have been carried out previously on BC rock types.

Elastic numerical modelling was carried out to illustrate the extents of tensile stress zones and extension zones around of typical BC mine excavations. The models showed that large zones of extension strain can occur around BC excavations, and that the magnitudes of the extension strain can substantially exceed the critical values determined from the laboratory testing. The implication of this is that there are substantial zones surrounding BC mine excavations that will be prone to time-dependent spalling conditions and perhaps more significant failure.

Keywords

tensile strength, creep, time-dependent failure, rock strength, Bushveld Complex.

Introduction

South Africa is a major mining country and is host to a significant proportion of the world's mineral resources. Gold resources in South Africa occur mainly in the Witwatersrand Basin, and platinum group metals (PGMs) in the Bushveld Complex (BC). The nation hosts most of the world's mineral reserves of platinum and palladium, about 75% and 50% respectively (Cawthorn, 1999), and future production potential is estimated to be more than a hundred years. Furthermore, Cawthorn (1999) suggests that, since mining of PGMs has progressed only to an average depth of 2000 m below surface, the proven reserves may easily double as deeper exploration and mining take place.

The 2060 Ma Bushveld Complex is an irregular, saucer-shaped massive layered igneous intrusion (Figure 1), with outcrop extremities of approximately 450 km east–west and 300 km north–south (Simmat *et al*., 2006). The platinum reserves occur in three horizons: the Merensky Reef, the Upper Group 2 (UG2) Reef, and the Platreef (Cawthorn, 1999; Cawthorn and Boerst, 2006). Below these reef horizons lies the Upper Group 1 (UG1) Reef, the platinum content of which has not yet been widely proven to be economically viable. The continuity of the Merensky and UG2 reefs has been confirmed to 3000 m below surface (Cawthorn, 1999). Potholes, faults, and dykes in the Merensky and UG2 reefs disrupt the otherwise uniformly shallow dipping and narrow tabular reef characteristics peculiar to the BC mines.

The main rock types associated with the Merensky and UG2 reefs are gabbro, norite, anorthosite, and pyroxenite. 'The [Merensky] reef in its most common form is a pegmatoidal (coarse-grained) feldspathic pyroxenite, generally bounded by thin (approx. 20 mm) chromitite layers. The immediate hangingwall is pyroxenite, 1–5 m thick, which grades upwards through norites to anorthosites. The footwall generally consists of various types of norite and anorthosite, and less commonly feldspathic pyroxenite or harzburgite, which however often forms the immediate footwall of pothole reefs' (Rangasamy, 2010). Anorthosite is an important rock type in the BC. As indicated by Barnes and Maier (2002),

* *Anglo American Platinum Ltd and School of Mining Engineering, University of the Witwatersrand.*

† *School of Mining Engineering, University of the Witwatersrand.*

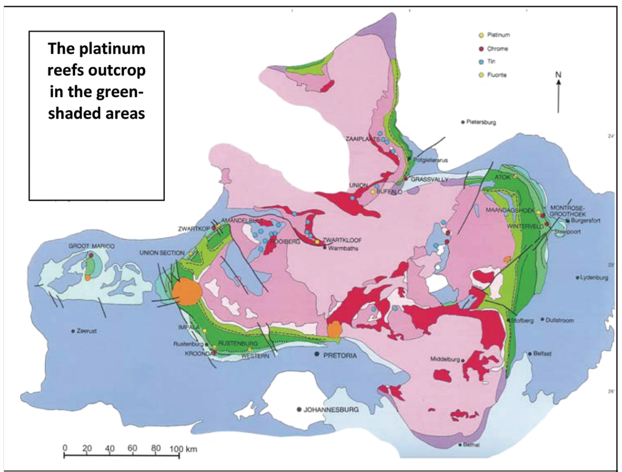

Figure 1—Geological map of the Bushveld Complex (after Viljoen and Schürmann, 1998)

anorthosite is a brittle rock, and can therefore be expected to be prone to failure under tensile stress and extension conditions. They state, 'Mottled anorthosite refers to anorthosite in which large areas of inter-cumulus orthopyroxene and/or augite (from 10 mm diameter up to the diameter of tennis balls) form dark mottles in a matrix of pure white or pale grey anorthosite. Spotted anorthosite is anorthosite in which a small percentage of cumulus orthopyroxene gives the effects of dark spots in the pale anorthosite matrix.'

In situ stress conditions are very important influences on the behaviour of mining excavations in the BC. Relevant information from a database of *in situ* stress measurements across southern Africa (Stacey and Wesseloo, 2004) are summarized in Figure 2. High horizontal to vertical stress ratios (2.5–4 in the pseudo-strike direction) are commonly experienced at shallow depths in BC mines. At greater depths of about 1000 m, the stress ratios are lower, in the region of 1 to 1.5.

Mining operations in the Bushveld Complex

Underground mines contribute most of the PGM production in South Africa, the bulk of the ore currently being mined at depths between 500 m and 2000 m below surface. Primary and secondary excavations are mined to access the mineral reserves, and these have to remain open and stable for the life of the mine. In shallow BC mines, the compressive strength of the rock (UCS) is usually much greater than the compressive stress in the excavation walls. In these stress conditions, failure of rock would not be expected. However, stress-induced spalling of rock from walls of mining excavations is frequently observed (Ryder and Jager, 2002). Figure 3 illustrates this behaviour in a haulage tunnel at a depth of approximately 400 m below surface.

The walls of the haulage were observed to scale with the passage of time, implying time-dependent behaviour of the wallrock. This has been observed in the BC mines, between months and years after excavation, due to fracture initiation and propagation in intact rock. Time-dependent stope closure behaviour in BC stopes has also occurred (Malan *et al.*, 2007). Damage in excavation walls in BC mines is exacerbated by the intersection of fractures with naturally-occurring, shallow-dipping discontinuities and layered rock, resulting in the formation of blocks of rock with high fallout and unravelling potential. Instability problems in inclined shafts and in dip-oriented tunnels have occurred in some mines in the Rustenburg mining environment, as evidenced by observed roof failures and resulting 'gothic arches' in tunnels oriented on-dip (see Figure 4).

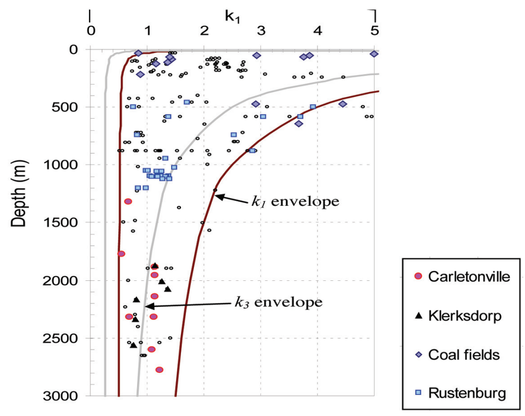

Figure 2—*In situ* stress data for South African mines (Stacey and Wesseloo, 2004)

Figure 3—Spalling in a haulage tunnel in a platinum mine, western limb, Bushveld Complex

Figure 4—Stress-induced failure in the roof of a dip-oriented tunnel in a platinum mine (Stacey and Wesseloo, 2004)

Since rock strengths appear to be considerably greater than rock stresses, the observations indicate that rock failure might be considered to be somewhat unexpected. However, in other situations, rock in the walls of excavations has been observed to fracture or fail at stress levels well below the UCS, as found by Stacey and Yathavan (2003). They reviewed published information on the development of fractures at low stress levels in rock (Grimstad and Bhasin, 1997; Myrvang *et al*., 2000). This review showed that stress-induced failure can occur even when the maximum induced stresses are as low as one-quarter to one-half of the rock strength.

Ortlepp (1997) observed a rockburst in a sandstone roof of a shallow coal mine about 20 m below surface. These findings point to a different failure mechanism than the mechanisms commonly assumed in the Mohr-Coulomb and Hoek-Brown failure criteria. Observations of face-parallel slabbing or spalling at low confining stress suggest extension as a fracturing mechanism.

Stress and strain distributions around typical mining excavations

Since failure of rock around mining excavations at shallow depth is commonly observed, it was considered appropriate to carry out stress analyses to evaluate the magnitudes of stress and strain that might theoretically be expected. Numerical analyses of typical mining excavations, a stope and a stope pillar, were therefore carried out using k-ratios of 1 and 2, characteristic of the deeper and shallow mining respectively. Two mining depths were considered, 500 m and 1000 m below surface. Examples of computed minimum principal stresses (σ_3), including orientations, and minimum principal strains, around a typical in-stope pillar are shown in Figures 5 and 6.

Distributions of minimum principal stresses and strains around a typical stope excavation were also determined. Examples of the minimum principal stress and minimum principal strain distributions are shown in Figures 7 and 8.

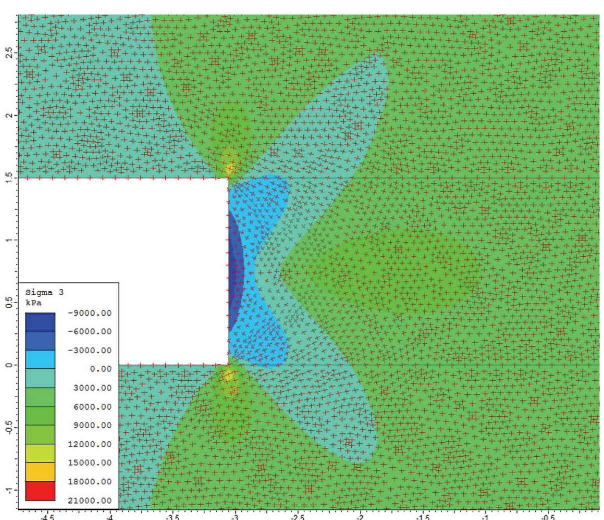

Figure 5—Distribution of minor principal stress (σ_3) around a pillar at a depth of 500 m, k-ratio of 2

Tensile stresses occur in the immediate sidewalls of the pillar, and in the stope hangingwall. The immediate peripheries of the excavations experience substantial zones of extension. Extension strains that exceed a critical extension strain value can indicate the initiation of fracturing in rock (Stacey, 1981). These fractures form in planes normal to the direction of extension strain, which corresponds with the direction of minimum principal stress (the least compressive principal stress). Importantly, extension can occur in an environment in which all three principal stresses

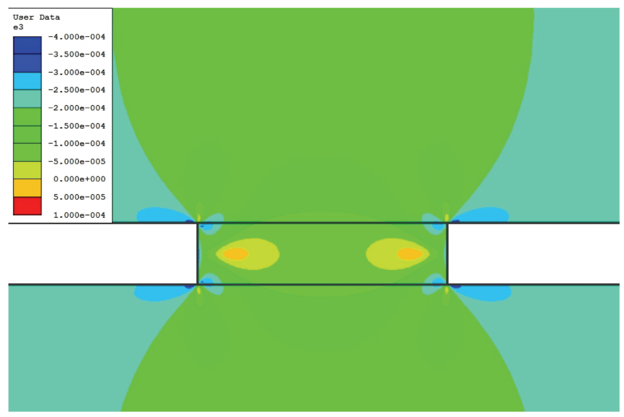

Figure 6—Distribution of minimum principal strain around a stope pillar at a depth of 500 m, k-ratio of 2

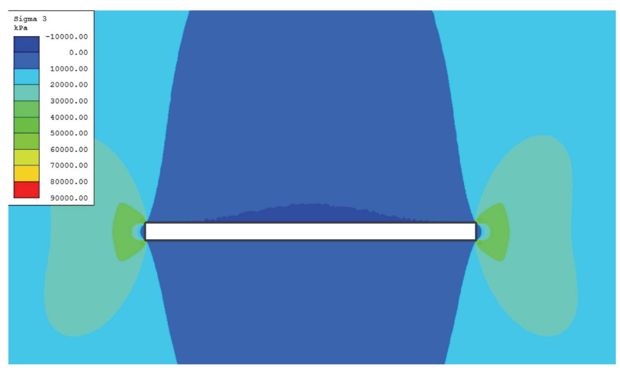

Figure 7—Minimum principal stress around a stope at a depth of 500 m, k-ratio of 2

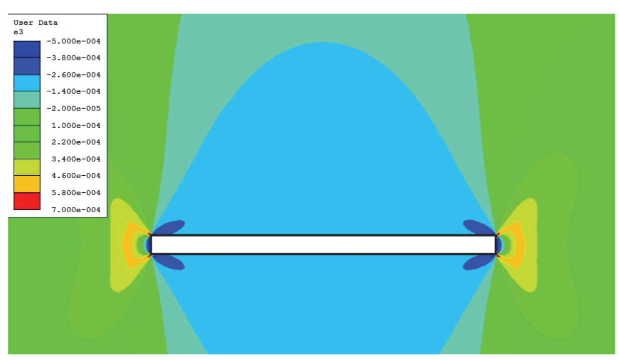

Figure 8—Minimum principal strain around a stope at a depth of 500 m, k-ratio of 2

are compressive. It is to be noted that, in the calculation of the minimum principal strain, the value of σ_2 used was based on the assumption of plane strain.

Observed hangingwall delamination has been attributed to the layered nature of the rocks. However, the effect of low confinement, as well as tensile and extension conditions, could be a direct or a contributory cause. The models indicate zones of extension strain and principal stress orientations that are compatible with the geometry of spalling observed in the excavation wall rock.

The photograph in Figure 9 shows a platinum mine stope that had been standing for at least 6 months. The hangingwall of the stope delaminated and face-parallel fractures, corresponding with the modelled principal stress orientations, developed slowly at stresses lower than the compressive or tensile strengths of the host rock types. Loose blocks form when the fractures propagate and intersect natural discontinuities, resulting in unravelling around support. Installed support in these conditions curbs the propagation of fractures, and slows down the manifestation of excavation wall damage.

Figure 9—Delamination of hangingwall in a platinum mine stope

Time-dependent behaviour of rock

When an excavation is mined, stress redistribution occurs around the opening, and a change in the stress field can result in significant deformation, or creep, occurring over a relatively long period of time. Creep is defined as increasing strain while the stress is held constant (Rinne, 2008) and is observed mainly in soft rocks, for example salt. However, all types of hard rock also exhibit creep characteristics over long enough time intervals (Critescu and Hunsche, 1998).

Creep commonly consists of three stages: after an instantaneous elastic strain when a constant load is applied, primary (transient) creep occurs; then, with time, secondary or steady state creep occurs; finally, tertiary or accelerating creep will occur, leading to eventual failure. The tertiary stage always terminates in fracture and establishes the link with the phenomenon of time-dependent failure (Wawersik, 1972). Drescher and Handley (2003) observed these creep stages when they carried out uniaxial compression creep tests on Ventersdorp lava and Elsburg quartzite.

According to Ryder and Jager (2002), the long-term strength of rock can be as low as 70% of the UCS. However, tests on granite and anorthosite by Schmidtke and Lajtai (1985) showed that stresses as low as 50% of the short-term strength almost certainly caused time-dependent stress-corrosion cracking in brittle rocks, severe enough to cause delayed failure. Investigations of crack growth in loaded granite using a scanning electron microscope indicated that new cracks developed continuously under constant load (Kranz, 1976). These findings point towards the importance of including time-dependent behaviour in the design of excavations in rock.

Ryder and Jager (2002) state that the creep rate in rock is dependent on the magnitude of the deviatoric stress (σ_1 - σ_3) and not the individual magnitudes of σ_1 and σ_3, (where σ_1 and σ_3 are the major and minor principal stresses respectively). However, orientations of fracturing due to deviatoric stresses would not correspond with the observed underground spalling or slabbing behaviour. In contrast, observations of failure, and the results of the numerical analyses described above, which show that large zones of rock around excavations are likely to be in a condition of extension, indicate that extension fracturing is a more likely mechanism. An investigation into the time-dependent characteristics of BC rock types was therefore considered to be justified.

Laboratory tests on Bushveld Complex rocks

Few studies have been conducted on the time-dependent behaviour of strong brittle rocks. Of significance for South African mining conditions is the testing described by Bieniawski (1967c; 1970), Kovács (1971), Drescher (2002), Drescher and Handley (2003), and Watson *et al.* (2009). However, these publications provide very little information on the time-dependent properties of BC rock types. Appropriate testing was therefore necessary to provide data for comparison with the results of the numerical analyses.

A range of laboratory rock strength tests was carried out on several BC rock types: UCS tests to establish the elastic properties and failure characteristics under uniaxial compression and, from the UCS test results, interpretation of long-term strength and stress and strain values observed at failure; Brazilian indirect tensile (BIT) tests (ISRM, 2007) to determine normal tensile strengths; and time-dependent BIT tests.

The following methodology was used to achieve the objectives outlined above:

- UCS tests on cylindrical specimens of several BC rock types prepared from different depth sections along a single vertical drill-hole core
- Normal BIT tests on several BC rock types
- Time-dependent constant hold-load BIT tests on several BC rock types stressed to pre-determined hold-load levels. The times-to-failure for the different test categories at constant load were recorded for the determination of time-dependent characteristics.

The UCS and BIT test specimens were prepared from the core of a single exploration drill-hole. The vertical borehole gives a good cross-sectional representation of the BC layering. Drill-hole core samples were taken from a zone up to 10 m above and below the hangingwall (HW) and footwall (FW) contacts of the Merensky (MR), Upper Group 1 (UG1). and Upper Group 2 (UG2) reef horizons.

Nine test specimen categories were identified: spotted anorthosite, mottled anorthosite (A, D, and I), pyroxenite, norite, anorthositic norite, and spotted anothositic norite (F and H).

UCS and BIT test specimens were cut alternately from the core to provide an unbiased sample representation for the two test methods. No two test specimens for the same test method were cut adjacent to one another. In total, 334 specimens were tested. The majority of test specimens were prepared for the BIT tests, and most of these were used in the time-dependent tests. For each test type, the numbers of specimens that were tested successfully with valid results varied.

All specimens were prepared and tested according to the ISRM Suggested Methods for rock testing (ISRM, 2007). The cores were BQ size with a diameter D = 36.3 mm. Average length to diameter ratios of 2.2 and 0.5 were achieved for the UCS and BIT test specimens respectively. Inspection showed that the specimens did not have visible pre-existing deformities. Circumferential and axial strain gauges were attached to the UCS test specimens to measure strains during the tests. All tests were carried out in anhydrous conditions at room temperature and pressure.

The data from the test results was processed and used to determine UCS values, and to plot stress-strain curves, similar to that shown in Figure 10. The average values of elastic properties of mottled anorthosite (A) are indicated on the plot. After initial nonlinear behaviour (possibly crack closure, Bieniawski, 1967a; 1967b), the plot shows largely linear behaviour up to the peak strength of the specimen.

The specimens failed in the typical fashion observed for brittle rock failure – initial axial extension fractures and ultimately shear, resulting in some cases, in conical end-pieces and a completely fractured or crushed middle portion.

Axial stress-volumetric strain plots were used to evaluate the 'long-term strength' of the rock types. According to Bieniawski (1967a), the 'nose' of the stress-volumetric strain plot marks the 'long-term strength' of the specimen. Long-term strengths were determined for each rock type and average values calculated. Variations in the test results are attributed to inherent variability in the rock specimens. A summary of the UCS test results, together with the 'long-term strength' values, is given in Table I.

The average value of the 'long-term strength' for the nine categories of rock types was 78 MPa, which is 56.4% of the UCS value of the rock types tested. The lowest long-term strength values were recorded for pyroxenite and mottled anorthosite at 44% of their respective UCS values.

Brazilian indirect tensile (BIT) tests

A servo-controlled rock testing machine was used to carry out normal and time-dependent BIT tests. A constant loading rate of 2 kN/min was used to load specimens, targeting failure in 3 to 4 minutes, depending on the sample's tensile strength. A summary of the results of the normal Brazilian tensile strength tests is presented in Table II (with elastic modulus values obtained from the UCS tests). On average, the tensile strength magnitude was found to be 5% (1/20) of the UCS of the same rock type.

Typical strain values at failure for each rock type were calculated based on the average elastic modulus of the rock type, and ranged from 0.16 to 0.21 millistrain, with an average value of 0.18 millistrain. This range agrees with published data; for comparison, the value obtained for norite was 0.173 millistrain (Stacey, 1981).

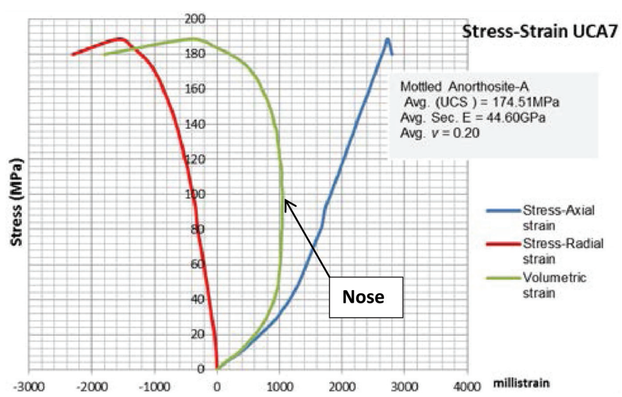

Figure 10—Example of a stress-strain graph for mottled anorthosite

Table I

Summary of average results from UCS tests

Rock type/ Code	Mottled anorthosite (A)	Spotted anorthositic (B)	Pyroxenite (C) norite	Mottled anorthosite (D)	Norite (E)	Spotted anorthositic norite (F)	Anorthositic norite (G)	Spotted anorthosite (H)	Mottled anorthosite (I)
Sample diameter, D (mm)	36.30	36.30	36.30	36.30	36.30	36.30	36.30	36.30	36.30
Sample length, L (mm)	80.74	84.79	81.66	81.13	83.71	82.87	80.99	81.03	80.98
L/D ratio	2.23	2.34	2.25	2.24	2.29	2.28	2.23	2.23	2.23
Sample mass, M (g)	231.41	254.20	270.30	230.93	261.32	248.10	253.48	237.80	232.32
Sample density, ρ (kg/m^3)	2769.46	2898.71	3198.41	2750.49	3016.40	2892.39	2990.22	2835.12	2772.17
Failure load, (kN)	180.60	139.40	129.80	140.50	96.00	154.60	114.00	159.60	182.20
UCS, σ_c (MPa)	174.51	134.70	125.42	135.76	92.76	149.38	110.15	154.22	176.05
Elastic modulus, E (GPa)	44.60	33.32	35.49	39.01	30.90	40.65	37.90	42.64	45.31
Poisson's ratio, v	0.20	0.21	0.17	0.28	0.19	0.21	0.15	0.22	0.19
Long-term strength (MPa)	90.2	61.8	56.5	59.75	53.5	75.6	83.6	103.33	125.75
% of UCS	57	46	44	44	57	51.4	72.4	67	68.75

Table II

Summary of normal BIT test results

Rock type	Sample ID	Sample diameter D (mm)	Sample thickness, *t* (mm)	t/D ratio	Sample mass, M (g)	Average load at failure, P (kN)	Average BIT strength, σ_t (MPa)	Average elastic modulus, E (GPa)	Average strain at failure, (millistrain)	Average time-to-failure (s)
Mottled anorthosite (A)	DBA	36.30	19.27	0.53	54.26	8.19	7.46	46.72	0.16	220.71
Spotted anorthositic norite (B)	DBB	36.30	18.88	0.52	55.46	6.84	6.35	33.32	0.19	205.72
Pyroxenite (C)	DBC	36.30	18.97	0.52	62.67	7.43	6.89	35.40	0.19	206.77
Mottled anorthosite (D)	DBD	36.30	18.77	0.52	53.84	6.83	6.38	39.01	0.16	138.02
Norite (E)	DBE	36.30	18.36	0.51	57.67	6.92	6.62	30.90	0.21	160.35
Spotted anorthositic norite (F)	DBF	36.30	18.61	0.51	55.24	8.27	7.76	40.65	0.19	138.17
Anorthositic norite (G)	DBG	36.30	17.65	0.49	56.31	7.71	7.65	37.90	0.20	203.85
Spotted anorthosite (H)	DBH	36.30	17.59	0.48	51.29	7.11	7.10	42.64	0.17	213.83
Mottled anorthosite (I)	DBI	36.30	17.06	0.47	48.93	6.82	7.04	45.31	0.16	214.03

Table III

Time-dependent test results

Rock type . specimen I.D	Mean BIT strength, Pmean (kN)	Static BIT test load, x% of P_{mean} (kN) and time-to-failure, *T* (s)									
		90%	Time, T (s)	85%	Time, T (s)	80%	Time, T (s)	75%	Time, T (s)	70%	Time, T (s)
A	8.19	7.37	268	6.96	972	6.55	11658	6.14	39831	5.73	111480
B	6.84	6.16	1587	5.81	2200	5.47	4578	5.13	19837	4.79	62226
C	7.43	6.69	16830	6.32	38695	5.94	33705	5.57	207423	5.20	23605
D	6.83	6.15	229	5.81	16328	5.46	82700	5.12	36306	4.78	151889
E	6.92	6.23	1652	5.88	375	5.54	10327	5.19	1679	4.84	60706
F	8.27	7.44	-	7.03	375	6.62	1705	6.20	2698	5.79	60709
G	7.71	6.94	643	6.55	147	6.17	-	5.78	2483	5.40	805
H	7.11	6.40	4214	6.04	12291	5.69	8168	5.33	67109	4.98	62350
I	6.82	6.14	6213	5.80	45191	5.46	33038	5.12	38993	4.77	39151

A Mottled anorthosite; B Spotted anorthositic norite; C Pyroxenite; D Mottled anorthosite; E Norite; F Spotted anorthositic norite; G Anorthositic norite; H Spotted anorthosite; I Mottled anorthosite

Time-dependent Brazilian indirect tensile (BIT) strength tests

Pre-determined load levels, derived from the tensile strength values determined in the normal BIT tests, were used in the time-dependent BIT strength tests. The load levels used represented 70%, 75%, 80%, 85%, and 90% of the corresponding tensile strength for each rock type: At each load level, tests were conducted on sets of five specimens for each test category. Loading of each test specimen was increased at a rate of 2 kN/min up to the required hold-load. The time-to-failure, *T*(s), was recorded for complete test runs where specimen failure was observed. Owing to limited availability of the testing machine, the time-dependent tests were limited to a maximum of three days. In a few cases, particularly in the low load tests at 70%, failure did not occur within three days, and in some cases the testing machine tripped due to overheating. Valid test results were therefore recorded only if the initial loading build-up was completed to the hold stage, the machine did not trip, and the test was completed within three days.

Some of the tests, particularly those at 90% of tensile strength, resulted in failure during the load application stage, *i.e.* before reaching the constant load phase. Other test runs with similar premature failure results were attributed to rock material variability.

The time-dependent test results for the nine rock types are summarized in Table III.

The individual test results showed scatter in the time-to-failure. A logarithmic trend line was fitted to the results for each type category, as shown in Figure 11. The minimum value indicated by the curve may be taken as the long-term tensile strength of the rock type. Similar graphs were produced for all the rock types to determine the time–to-failure trends.

It may be estimated from these results that the long-term tensile strengths of BC rocks are likely to be between 60% and 70% of the short-term tensile strength normally reported for laboratory tests. Since all mining excavations are long-term in the context of the duration of testing carried out, these lower strength values should be taken into account in design.

From these results the equivalent extension strains at failure were calculated, and these indicate that an average value for the critical extension strain is likely to be approximately 0.12 millistrain.

Summary of laboratory test results

From the range of strength tests carried out, the following key outputs have been summarized:

a) Average UCS values obtained for the BC rocks tested varied between 93 MPa and 176 MPa

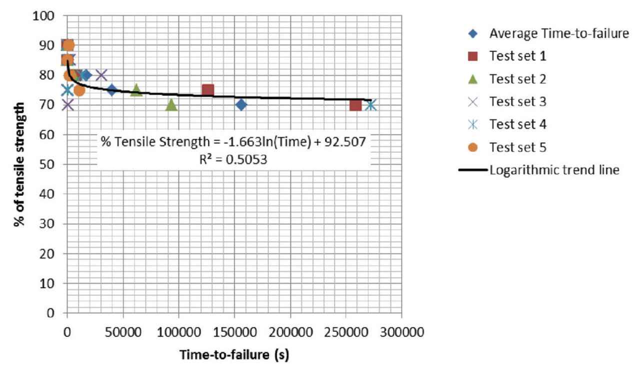

Figure 11—Time-to-failure plot for mottled anorthosite

b) The average long-term strength of the rocks (Bieniawski, 1967a), interpreted from the volumetric strain curves in the UCS tests, was 78 MPa, which is 56% of the UCS. The lowest long-term strength value obtained was 44% of the corresponding UCS value

c) Tensile strength magnitudes of the rocks were found to be between 4% and 7% of the UCS magnitudes (*i.e.* the tensile strength magnitude is about 1/20 of the UCS magnitude)

d) The minimum long-term tensile strengths of the rocks could not be determined owing to the limited testing duration of three days, but are certainly less than 70% of the short-term tensile strength normally reported for laboratory tests

e) Extension strain magnitudes at strength failure calculated from the normal tensile strength tests indicate a range of between 0.16 and 0.21 millistrain. Values corresponding with the long-term tensile strength would therefore be less than 70% of this range, *i.e.* 0.11 to 0.15 millistrain.

The extension strain magnitudes determined in the numerical modelling are significantly greater than those indicated in (e) above, the implication being that extension strain may be a suitable criterion for prediction of fracture and failure around BC mining excavations. Observations made in actual BC mine excavations revealed that fracturing of intact rock occurs over a protracted time, possibly due to the development and propagation of extension fractures, and that the manifestation of such fracturing was curbed by installed support.

Conclusions

The research described in this paper has dealt with the investigation of stress and strain conditions influencing the spalling of wallrock in mine excavations in the Bushveld Complex (BC). This involved laboratory testing of BC rocks in uniaxial compression and in indirect tension, including time-dependent indirect tension, as well as numerical modelling of typical mine excavations. The following conclusions are drawn:

- Observations made in BC mine excavations revealed that fracturing of intact rock occurs over a protracted time period, and that its manifestation is curbed by installed support
- There have been very few time-dependent or creep tests carried out in South Africa on BC rock types. The laboratory testing reported in this paper has provided new data in this regard
- The laboratory tests have shown that tensile strength magnitudes of BC rock types are approximately 5% of their compressive strength magnitudes
- The long-term uniaxial compressive strength of the BC rocks, interpreted from the axial stress-volumetric strain graph from the UCS test, is on average 78 MPa or 56% of the average UCS value
- The tensile strength of the BC rock types was found to be time-dependent. Failure times for individual test specimens showed large variability, but the general indication is that the time-dependent tensile strengths are between 60% and 70% of the tensile strength normally reported from laboratory testing, and possibly may even be less than 60%
- Extension strains calculated at tensile strength failure ranged between 0.16 and 0.21 millistrain. Values corresponding with the long-term tensile strength are less than 70% of this range, namely, less than 0.11 to 0.15 millistrain
- Numerical analyses of BC excavations were carried out, using elastic models and assuming homogeneity of material, to investigate the possible occurrence of zones in which tensile stresses and extension strains occur. The models showed that large zones of extension strain may occur around BC excavations, and that the magnitudes of the extension strain exceed the critical values determined from the laboratory testing. Predicted orientations of fracturing from these models correspond with observed geometry of spalling in excavations. The implication is that there are likely to be substantial zones surrounding BC mine excavations that will be prone to spalling conditions and perhaps more significant failure.

Acknowledgements

Impala Platinum is thanked for provision of the borehole core and associated information on which the research described in this paper was based. Joseph Muaka is thanked for assistance with numerical analyses specifically for the paper. The input of the second author is based on research supported in part by the National Research Foundation of South Africa (Grant-specific unique reference number (UID) 85971). The Grantholder acknowledges that opinions, findings, and conclusions or recommendations expressed in any publication generated by the NRF-supported research are that of the author(s), and that the NRF accepts no liability whatsoever in this regard.

References

BARNES, S-J. and MAIER, W.D. 2002. Platinum-group element distribution in the Rustenberg layered suite of the Bushveld Complex South Africa. The *Geology, Geochemistry, Mineralogy and Mineral Beneficiation of Platinum-Group Elements*. Special Volume 54, Canadian Institute of Mining and Metallurgy, Ottawa, Ontario. pp. 431–458.

BIENIAWSKI, Z.T. 1967a. The mechanism of brittle fracture of rock. *International Journal of Rock Mechanics and Mining Sciences*, vol. 4. pp. 396–435.

BIENIAWSKI, Z.T. 1967b. Mechanism of Brittle of Rock, Part 2. South African Council for Scientific and Industrial Research (CSIR). *Institute – Technology and Engineering*, Pretoria. p. 452.

BIENIAWSKI, Z.T. 1967c. Mechanism of Brittle of Rock, Part 3. South African Council for Scientific and Industrial Research (CSIR). *Institute – Technology and Engineering*, Pretoria. p. 452.

BIENIAWSKI, Z.T. 1970. Time-dependent behaviour of fractured rock. *Rock Mechanics*, vol 2. pp 123–137.

CAWTHORN, R.G. 1999. The platinum and palladium resources of the Bushveld Complex. *South African Journal of Science*, vol. 95, no. 11/12. p. 481–489.

CAWTHORN, R.G. and BOERST, K. 2006. Origin of the pegmatite pyroxenite in the Merensky unit, Bushveld Complex South Africa. *Journal of Petrology*, vol. 47, no. 8. pp. 1509–1510.

CRITESCU, N. D. and HUNSCHE, U. 1998. Time Effects in Rock Mechanics. Series in Materials Modeling and Computation. Wiley, Chichester, UK.. ISBN 0471 955175.

DRESCHER, K. 2002. An investigation into the mechanics of time-dependent deformation of hard rocks. MSc dissertation, Faculty of Engineering, University of Pretoria, Pretoria.

DRESCHER, K. and HANDLEY, M.F. 2003. Aspects of time-dependent deformation in hard rock at great depth. *Journal of the South African Institute of Mining and Metallurgy*, vol. 103, no. 5. pp. 325.

GRIMSTAD, E. and BHASIN, R. 1997. Rock support in hard rock tunnels under high stress. *Proceedings of the International Symposium on Rock Support – Applied Solutions for Underground Structures*, Lillehammer, Norway, 22–25 June 1997. Broch, E., Myrvang, A., and Stjern, G. (eds.). Norwegian Society of Chartered Engineers. pp 504-513.

ISRM. 2007. The Complete ISRM Suggested Methods for Rock Characterisation, Testing and Monitoring: 1974-2006. Ulusay, R. and Hudson, J.A. (eds). Compilation arranged by the ISRM Turkish National Group, Ankara, Turkey.

KOVÁCS, I.K.A. 1971. An investigation of the time-dependent behaviour of solid rock in uniaxial compression. *Report* MEG 1032. National Mechanical Engineering Research Institute, Council for Scientific and Industrial Research, Pretoria, South Africa.

KRANZ, R.L. 1976. Crack growth and development during creep of Barre granite. *International Journal of Rock Mechanics and Mining Sciences and Geomechanical Abstracts*. vol. 16. pp. 23–35.

MALAN, D.F., NAPIER, J.A.L., and VAN JANSE RENSBURG, A.L. 2007. Stope deformation measurements as a diagnostic measure of rock behaviour: a decade of research. *Journal of the Southern African Institute of Mining and Metallurgy*, vol 107, no. 11. pp. 743–765.

MYRVANG, A.M., ALNAES, L., HANSEN, S.E., and DAVIK, K.I. 2000. Heavy spalling problems in road tunnels in Norway – long time stability and performance of sprayed concrete as rock support. *Proceedings of the International Symposium on Rock Support – Applied Solutions for Underground Structures, Lillehammer*, Norway. Broch, E., Myrvang, A., and Stjern, G. (eds). Norwegian Society of Chartered Engineers. pp. 751–764.

ORTLEPP, W.D. 1997. Rock fracture and rockbursts – an illustrative study. *South African Institute of Mining and Metallurgy*, Johannesburg. 255 pp.

RANGASAMY, T.R. 2010. IMP03: Geotechnical report, Impala 18#. Unpublished company report, Middindi Consulting (Pty) Ltd.

RINNE, M. 2008. Fracture mechanics and subcritical crack growth approach to model time-dependent failure in brittle rock. PhD thesis, Faculty of Engineering and Architecture, Dept. of Civil and Environmental Engineering, Helsinki University of Technology, Helsinki.

RYDER, J.A. and JAGER, A.J. 2002. A Textbook on Rock Mechanics for Tabular Hard Rock Mines. Safety in Mines Research Advisory Committee (SIMRAC), Johannesburg.

SCHMIDTKE, R.H. and LAJTAI, E.Z. 1985. The long-term strength of Lac du Bennet granite. *International Journal of Rock Mechanics and Mining Sciences and Geomechanical Abstracts*, vol. 22. pp. 461–465.

SIMMAT, C.M., HERSELMAN, P. LE R., RÜTSCHLIN, M., MASON, I.M., and CLOETE, J.H. 2006. Remotely sensing the thickness of the Bushveld Complex UG2 platinum reef using borehole radar. *Journal of Geophysics and Engineering*, vol. 3. pp. 43 – 49.

Stacey, T.R. 1981. A simple extension strain criterion for fracture of brittle rock. *International Journal of Rock Mechanics and Mining Sciences and Geomechanical Abstracts*, vol. 18, no. 6. pp. 469–474.

STACEY, T.R. and WESSELOO, J. 2004. Updated stress database for South Africa. *Proceedings of the International Symposium on In-situ Rock Stress*, Trondheim, Norway, 19–21 June 2006. Lu, M. Li, C.C., and Dalde, H. (eds.) Taylor and Francis, London. pp. 46–471.

STACEY, T.R. and YATHAVAN, K. 2003. Examples of fracturing of rock at very low stress levels. ISRM – Technology Roadmap for Rock Mechanics. *South African Institute of Mining and Metallurgy*, Johannesburg.

VILJOEN, M J. and SCHÜRMANN, L.W. 1998. Platinum-group metals. *The Mineral Resources of South Africa*. Wilson, M.G.S. and Anhaeusser, C.R. (eds.). Council for Geoscience, Pretoria. pp. 532–568.

WATSON, B.P., KUIPERS, J.S., HENRY G., PALMER, C.E., and RYDER JA. 2009. Nonlinear rock behaviour and its implications for deeper level platinum mining. *Journal of the Southern African Institute of Mining and Metallurgy*, vol. 109, no. 1. pp. 5–9.

Wawersik, W.R. 1972. Time-dependent rock behaviour in uniaxial compression. *Proceedings of the 14th US Symposium on Rock Mechanics (USRMS)*, University Park, Pennsylvania, 11–14 June, 1972, American Society of Civil Engineers. pp. 85–106. ◆